

# Decline in Thermal Habitat Conditions for the Endangered Delta Smelt as Seen from Landsat Satellites (1985–2019)

Gregory H. Halverson,\* Christine M. Lee, Erin L. Hestir, Glynn C. Hulley, Kerry Cawse-Nicholson, Simon J. Hook, Brian A. Bergamaschi, Shawn Acuña, Nicholas B. Tuffiaro, Robert G. Radocinski, Gerardo Rivera, and Ted R. Sommer



Cite This: <https://doi.org/10.1021/acs.est.1c02837>



Read Online

ACCESS |



Metrics & More

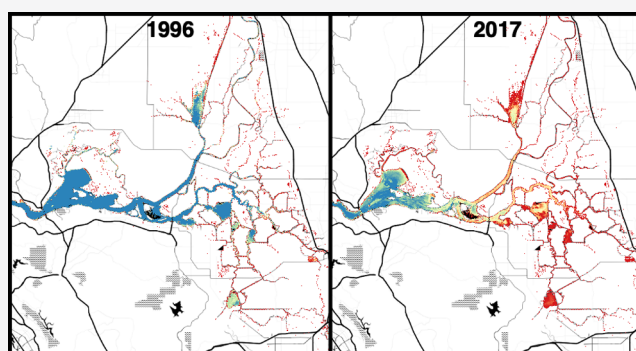


Article Recommendations



Supporting Information

**ABSTRACT:** This study uses Landsat 5, 7, and 8 level 2 collection 2 surface temperature to examine habitat suitability conditions spanning 1985–2019, relative to the thermal tolerance of the endemic and endangered delta smelt (*Hypomesus transpacificus*) and two non-native fish, the largemouth bass (*Micropterus salmoides*) and Mississippi silverside (*Menidia beryllina*) in the upper San Francisco Estuary. This product was validated using thermal radiometer data collected from 2008 to 2019 from a validation site on a platform in the Salton Sea (RMSE = 0.78 °C,  $r = 0.99$ ,  $R^2 = 0.99$ ,  $p < 0.01$ , and  $n = 237$ ). Thermally unsuitable habitat, indicated by annual maximum water surface temperatures exceeding critical thermal maximum temperatures for each species, increased by 1.5 km<sup>2</sup> yr<sup>-1</sup> for the delta smelt with an inverse relationship to the delta smelt abundance index from the California Department of Fish and Wildlife ( $r = -0.44$ ,  $R^2 = 0.2$ ,  $p < 0.01$ ). Quantile and Theil–Sen regression showed that the delta smelt are unable to thrive when the thermally unsuitable habitat exceeds 107 km<sup>2</sup>. A habitat unsuitable for the delta smelt but survivable for the non-natives is expanding by 0.82 km<sup>2</sup> yr<sup>-1</sup>. Warming waters in the San Francisco Estuary are reducing the available habitat for the delta smelt.



**KEYWORDS:** delta smelt, habitat compression, pelagic organism decline, water surface temperature, remote sensing

## INTRODUCTION

Water surface temperature (WST) is one of the most critical aspects of coastal water quality and aquatic habitat. Recent global increases in temperature are expected to continue rising in the coming decades and centuries.<sup>1</sup> WST is an important factor in the biological activity of coastal processes, and assessing ecosystem changes with remote sensing data is an effective way to track change systematically over large spatial extents.<sup>2</sup> Landsat is of particular interest for inland and coastal WST monitoring because it provides the fine spatial resolution (60–120 m) needed to resolve complex inland and coastal water bodies.<sup>3</sup> Furthermore, recent advances in surface temperature retrievals provide accurate, calibrated products that provide us with a multidecadal surface temperature time series that present new opportunities to assess estuarine surface water temperature.<sup>4</sup>

The San Francisco Estuary (SFE) watershed (Figure 1), which drains more than 40% of California, is central to California's water supply system.<sup>5–7</sup> As one of the largest estuaries on the west coast of North America, half of California's stream-flow transits through the SFE, and the system is the hub of federal, state, and local water projects that supply water to over a million hectares of agriculture and

nearly 30 million people.<sup>8</sup> The SFE is also a major biodiversity hotspot, providing habitat to a number of endemic and native species.<sup>9</sup> Half of California's migrating waterfowl and two-thirds of the state's salmon runs depend on the SFE.<sup>10</sup>

The SFE has been extensively developed, including the construction of over 1100 miles of levees and conveyance structures, conversion of wetlands into agriculture, and large-scale urbanization.<sup>11</sup> These changes are further compounded by other ecological stressors, such as climate change,<sup>12</sup> sea level rise,<sup>13</sup> invasive species,<sup>14,15</sup> contaminants,<sup>16</sup> water diversions,<sup>17</sup> and altered hydrology,<sup>18</sup> which have all contributed to detrimental ecosystem impacts.

The delta smelt, *Hypomesus transpacificus*, is one of the iconic native and endangered species of the SFE. The delta smelt are symbolic of the competing needs placed on this

Received: April 30, 2021

Revised: November 7, 2021

Accepted: November 12, 2021

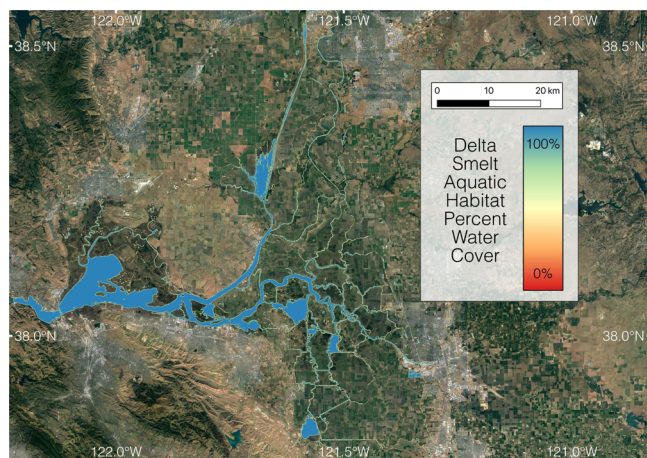


**Figure 1.** Map of critical delta smelt habitat according to the United States Fish and Wildlife Service displayed as percent water cover from 120 m convolution of the C-CAP land cover classification.<sup>19</sup>

fragile and diverse ecosystem. This fish has experienced a continued decline in the 1980s and another sustained decline starting in 2002, known as the pelagic organism decline (POD), from which it has not recovered.<sup>20,21</sup> For example, since 2018, zero delta smelt have been recorded during the California Department of Fish and Wildlife Fall Midwater Trawl, a primary measurement of long-term population trends. Although, limited numbers of fish are still collected in some other surveys. The delta smelt are highly sensitive to changes in water quality conditions, including temperature,<sup>22</sup> salinity,<sup>23</sup> and turbidity.<sup>17,23,24</sup> Habitat compression is expected under climate change,<sup>25</sup> along with an increase in the number of days with stress and mortality associated with worsening thermal conditions for the delta smelt.<sup>12,26</sup>

Surface temperature has been a fundamental variable observed by satellite-based earth observing systems. Long-term satellite records of surface temperatures have provided key insights into long-term trends in global warming.<sup>27</sup> The addition of higher resolution thermal bands included in Landsat 5 and beyond have provided the spatial resolution needed to resolve local and regional scale changes over more recent decades. This study combines a 35 year record of WST and thermal tolerance data from prior laboratory-controlled studies to examine changes in thermal habitat availability for the delta smelt and two non-native fish. This investigation addresses two key research questions:

1. How has WST changed in the SFE over the last 35 years?
2. What are the implications of temperature changes on thermal habitat availability for the endangered delta smelt, as compared to non-native species?

## DATA AND METHODS

**Landsat Surface Temperature.** The Landsat series of satellites have been placed into low earth orbit (LEO) with a consistent overpass time of 10:30 ± 15 min AM (local time). This series provides a consistent 35 year record of changes for the mid-morning WST, with no major sensor drift.<sup>28–30</sup> This study used the full record of surface temperature images acquired by Landsat 5, 7, and 8 over the SFE at path/row 044/033 and 044/034 from 1985 to 2019. Level 2 collection 2 data were acquired as 30 m rasters using the Earth Explorer API.<sup>31</sup>

Three Landsat acquisitions covering the SFE appeared to have geolocation issues and had to be removed: Landsat 7 on 2014-05-01, Landsat 5 on 2008-06-5, and Landsat 7 on 2010-08-06. The Landsat 5 120 m, Landsat 7 60 m, and Landsat 8 100 m thermal images are all resampled to 30 m images and provided as atmospherically corrected surface temperature in collection 2. A time series of 039/037 was also retrieved from 2008 to 2019 for validation at the Salton Sea site.

**Water Surface Temperature Masking and Land/Water Unmixing.** The full record of Landsat surface temperature was masked to WST for the spatial monitoring of the aquatic habitat. To identify water pixels, we utilized the Coastal Change Analysis Program (C-CAP) regional land cover dataset from the National Oceanic and Atmospheric Administration (NOAA). The C-CAP dataset provides Landsat-based land cover classification at 30 m spatial resolution and forms the coastal counterpart to the National Land Cover Database (NLCD) but makes more detailed distinctions between estuarine land cover types. We considered only pixels with the open water code of 21 to be water, exclusive of estuarine and palustrine classes. We projected each of the 044/033 and 044/034 images onto the grid of C-CAP open water pixels within the United States Fish and Wildlife Service boundary of the delta smelt critical habitat (Figure 1).<sup>19</sup>

To account for mixed land/water pixels in the 30 m Landsat images of temperature, we used a land/water unmixing strategy inspired by Martí-Cardona et al. 2019.<sup>32</sup> We up-sampled the 30 m water pixel mask, with zero representing land and one representing water, to a 120 m grid by average as a continuous variable to simulate percent water cover at the native resolution of the Landsat 5 thermal sensor, the coarsest of the three Landsat satellites used here. We then cubically down-sampled that percent water cover image back to the 30 m analysis grid to generate a 30 m percent water cover image. We considered pixels with greater than 95% water cover to be the lower bound in the spatial extent of the aquatic habitat, covering 230 km<sup>2</sup>. We used the percent water cover at each 30 m pixel as a set of weights for habitat area quantification, covering 329 km<sup>2</sup>. We considered the original 30 m C-CAP land cover classification to represent an upper bound in the spatial extent of the aquatic habitat on the 30 m grid, covering 386 km<sup>2</sup>. The percent water cover map for the delta smelt aquatic habitat is displayed in Figure 1.

**Water Surface Temperature Validation.** Landsat WST retrievals were validated using surface temperature ( $T_s$ ) measurements from a platform-mounted radiometer deployed at the Salton Sea (SS1) validation site.<sup>33</sup>  $T_s$  is defined as the temperature at the top 10–500 μm of the water surface.<sup>34</sup> The time frame for validation spans from December 2008 to February 2019, for which there were available data. In each Landsat WST image, the corresponding Landsat WST value was taken as the mean of values within a 3 × 3 neighborhood of 30 m pixels surrounding the nearest pixel to the ground site. The Landsat WST was compared with in situ  $T_s$  using Pearson, Spearman, and Kendall correlation, root mean square error (RMSE), and ordinary least squares (OLS) coefficient of determination  $R^2$ .

**Fall Midwater Trawl Abundance Index.** The Fall Midwater Trawl Survey (FMWT) conducted by the California Department of Fish and Wildlife (CDFW) samples the delta smelt abundance at 122 stations in the SFE, ranging from San Pablo Bay to Stockton on the San Joaquin River, Hood on the

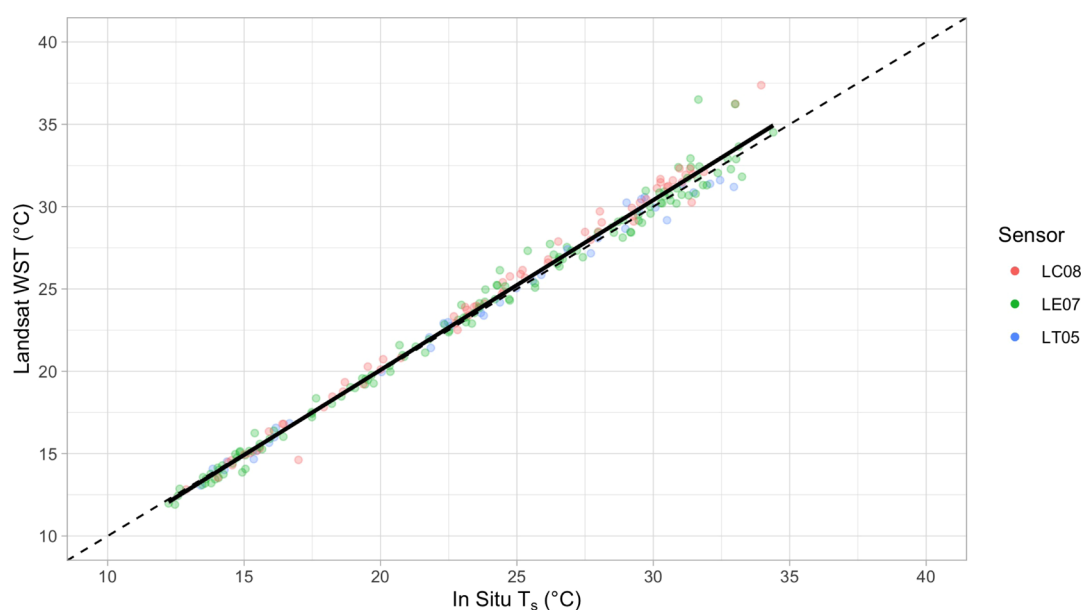


**Figure 2.** Scatter-plot of Landsat WST compared to  $T_s$  measurements from the Salton Sea validation site.

Sacramento River, and the Sacramento Deep Water Ship Channel.<sup>35</sup> Abundance sampling takes place for nine days each month from September to December each year. A subset of these data is used to calculate an annual abundance index. The FMWT has sampled smelt abundance in the SFE every year since 1967 (with the exception of 1974 and 1979). The data record of this measurement is continuous since 1980, covering the temporal availability of the Landsat 5, 7, and 8 WST record for comparison. Monthly abundance indices and annual totals for the delta smelt were retrieved from the CDFW.<sup>36</sup> The record of the delta smelt total abundance index was then used to examine changes in abundances relative to the WST trends and thermally unsuitable habitat (TUH). Table S3 provides a summary of the abundance indices used in this study.

**Thermally Unsuitable Habitat.** Changes in thermal habitat suitability were evaluated by quantifying the area of aquatic habitat that exceeds the critical thermal maximum temperature ( $CT_{max}$ ) of three fish species, the delta smelt and two non-native species, the largemouth bass (*Micropterus salmoides*) and Mississippi silverside (*Menidia berylina*).  $CT_{max}$  is the upper temperature tolerance of a fish, or an indicator of its ability to survive in a given water temperature.<sup>22</sup> The  $CT_{max}$  values used in this study were obtained from laboratory measurements in Davis et al. 2019 (Table S1).<sup>22</sup> Although the laboratory study measured exposure to multiple days of increased temperature and the revisit time of concurrent Landsat satellites is eight days, we refer to the laboratory-observed thermal tolerances for the three species of interest to spatially characterize the aquatic habitat based on the distribution of temperatures captured across the year. The delta smelt have the lowest thermal tolerance at 28.6 °C, followed by the largemouth bass (33.3 °C) and the Mississippi silverside (34.1 °C).<sup>22</sup> In the SFE ecosystem, although, the delta smelt are rarely found at temperatures above 24 °C.<sup>25</sup>

For each year in the Landsat record from 1985 to 2019, we aggregated all available Landsat images by maximum to generate an image of the annual maximum WST. For each annual maximum WST image, the area of TUH was determined by counting the number of pixels that exceeds  $CT_{max}$  for each image date for each species. The area of habitat

quantified for each pixel was weighted by percent water cover, between 0 m<sup>2</sup> for 0% water pixels and 900 m<sup>2</sup> for 100% water pixels. Lower bound estimates were quantified by limiting these pixel counts to >95% water cover pixels and counting these pixels as 900 m<sup>2</sup>. Upper bound estimates were quantified by counting all pixels classified as water by the C-CAP and exceeding species-dependent  $CT_{max}$  as 900 m<sup>2</sup> each. We examined the trend in the spatial median of the annual maximum surface temperature ( $WST_{max}$ ) with the more conservative set of >95% water cover pixels. These TUH values are summarized for all three fish species,  $TUH_{smelt}$ ,  $TUH_{bass}$ , and  $TUH_{silverside}$ , in Table S3, along with  $WST_{max}$  and the delta smelt abundance index, in the Supporting Information. We tested the trends in the TUH for all four variables,  $TUH_{smelt}$ ,  $TUH_{bass}$ ,  $TUH_{silverside}$ , and  $TUH_{competing}$ , using the Mann–Kendall trend test, ordinary least squares (OLS) regression, and Theil–Sen regression.

The relationship between the TUH and the delta smelt abundance index was examined using Theil–Sen, OLS, and quantile regression, and a nonparametric correlation hypothesis test. OLS regression was used to assess how the variance in the mean delta smelt abundance index is related to the variance in mean WST-based metrics. However, the thermal tolerance of fish is likely not best described by variance in means, but rather as a limiting factor to abundance. That is, it was expected that lower abundance indices would covary with increases in thermally unsuitable conditions, but it was not necessarily expected that thermally favorable or suitable conditions correspond with high abundance index values. This limiting relationship was examined using quantile regression.<sup>37</sup> Finally, Kendall's rank correlation coefficient (Kendall's  $\tau$ ), a nonparametric measure of relationships between ranked pairs, was used to test for distribution-free statistical dependence between  $TUH_{smelt}$  and the delta smelt abundance index.

## RESULTS AND DISCUSSION

**Validation at the Salton Sea Platform.** Comparison of WST retrievals of Landsat 5, 7, and 8 corresponding to radiometer measurements at the Salton Sea site showed good

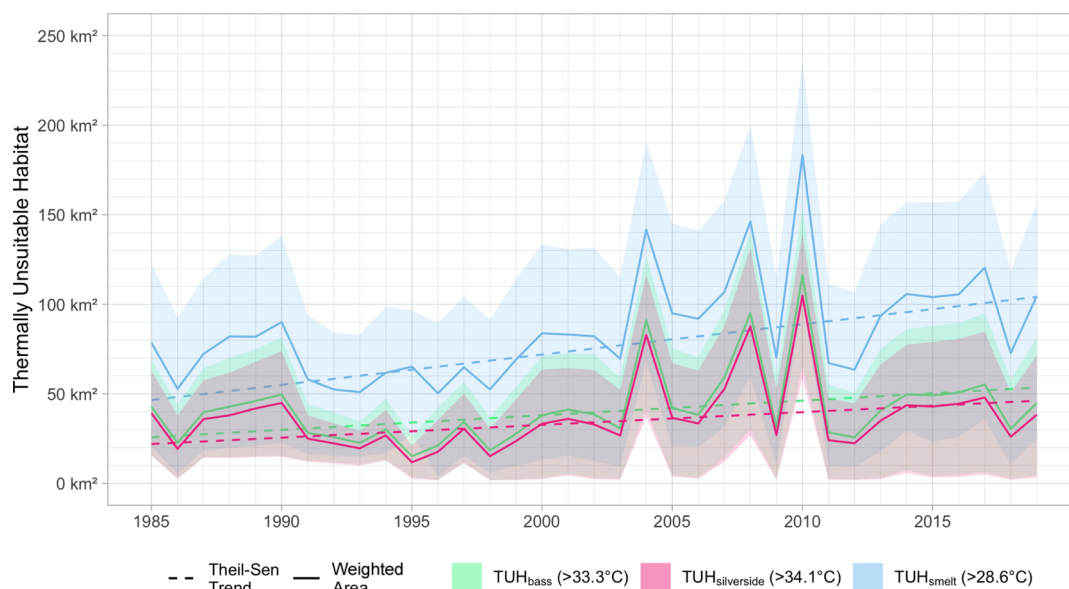


**Figure 3.** Timeline of  $TUH_{smelt}$ ,  $TUH_{bass}$ , and  $TUH_{silverside}$  with the weighted habitat area as solid lines, upper and lower bounds of land/water unmixing as ribbons and dashed Theil–Sen trend lines.

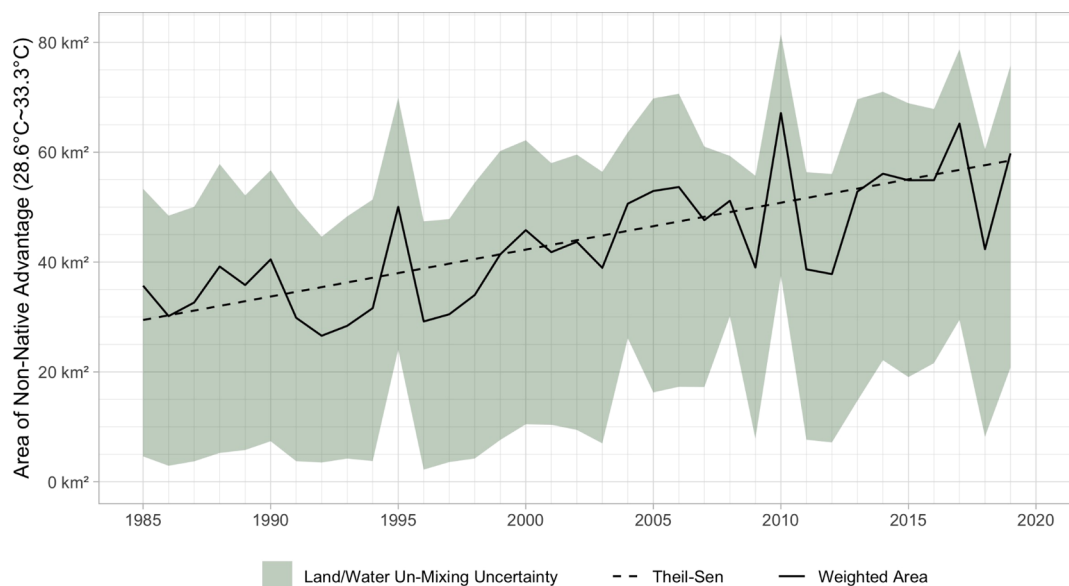


**Figure 4.** Timeline of  $TUH_{competing}$  with weighted habitat area quantification as the solid line, upper and lower bounds from land/water unmixing displayed by the ribbon, and increasing trend displayed as the dashed Theil–Sen line.

RMSE (0.78 °C), coefficient of determination ( $R^2 = 0.99$ ,  $p < 0.01$ ,  $n = 237$ ), and high correlation ( $r = 0.99$ ) (Figure 2, Table S2). Temperatures in this comparison ranged from 12 to 34 °C, which spans the range of conditions relevant to the delta smelt and other fish species under consideration in this study. The accuracy within one degree seen in this comparison gives confidence to the remotely sensed temperatures used to quantify habitat in this study.

**Thermally Unsuitable Habitat.** The rate of increase in  $TUH_{smelt}$  over the 35 year record was  $1.5 \text{ km}^2 \text{ yr}^{-1}$  (Theil–sen  $p < 0.01$ ), with a significant trend according to Mann–Kendall ( $\tau = 0.39$ ,  $p < 0.01$ ). The period of time from 1992 to 1996 shows the smallest  $TUH_{smelt}$  surface area, around  $50 \text{ km}^2$   $TUH$ , and the largest  $TUH$  areas in 2008 and 2017, reaching  $109 \text{ km}^2$  and  $120 \text{ km}^2$  (Table S3, Figure 3). The Theil–Sen trends were also significant for  $TUH_{bass}$  and  $TUH_{silverside}$ , but with smaller

slopes of  $0.6 \text{ km}^2 \text{ yr}^{-1}$  for  $TUH_{bass}$  ( $p < 0.01$ ) and  $0.42 \text{ km}^2 \text{ yr}^{-1}$  for  $TUH_{silverside}$  ( $p < 0.01$ ).

To evaluate the change in unsuitable habitat relative to the non-native fish, we also examined  $TUH_{competing}$ , the area where the higher thermal tolerances of the non-native fish may give them an advantage over the delta smelt (Figure 4).  $TUH_{competing}$  represents the area of habitat with the WST lower than  $CT_{bass}$  and  $CT_{silverside}$  ( $<33.3 \text{ }^\circ\text{C}$ ) but higher than  $CT_{smelt}$  ( $>28.6 \text{ }^\circ\text{C}$ ).  $TUH_{competing}$  was  $36 \text{ km}^2$  at the beginning of the Landsat record in 1985, and nearly doubled to  $60 \text{ km}^2$  in 2019.  $TUH_{competing}$  reached its maximum of  $65 \text{ km}^2$  in 2017. There was an increasing trend in  $TUH_{competing}$  of  $0.82 \text{ km}^2 \text{ yr}^{-1}$  ( $p < 0.01$ ) according to Theil–Sen regression (Figure 4).

This work observes increases in  $TUH$  conditions over the last 35 years (1985–2019), which is consistent with other work that finds that increasing water temperatures are

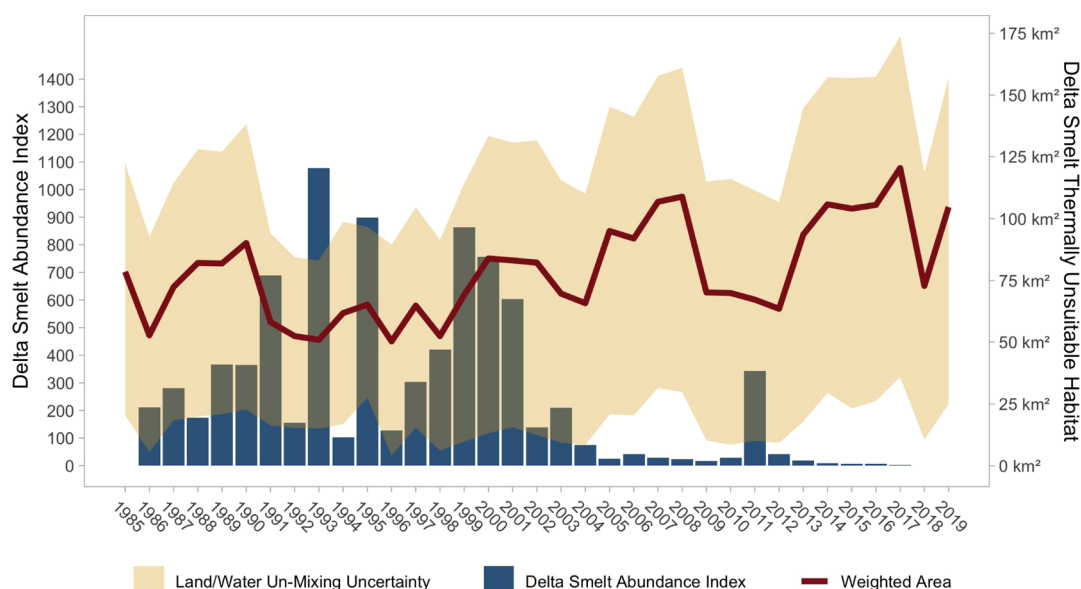


**Figure 5.** Timeline of delta smelt abundance index and  $TUH_{\text{smelt}}$  with the weighted habitat quantification as the solid line, and upper and lower bounds of land/water unmixing as the ribbon.

expected, and that will likely result in greater threats to the delta smelt.<sup>12</sup> However, to our knowledge, our estimates of habitat trends are the first empirical data demonstrating that the SFE is experiencing significant warming and the first to use high-resolution remote sensing to quantify the effects of this warming on the delta smelt habitat (Figure 5). Wagner and colleagues observed that, under climate change projections, the frequency of days that will have water temperature conditions that can cause mortality will increase.<sup>26</sup> Likewise, Brown and colleagues also show a compounding effect of degrading habitat conditions resulting in overall habitat compression for the delta smelt, accounting for turbidity, salinity, and temperature.<sup>38</sup> In fact, projected water temperatures in particular were called out as the dominant factor resulting in near total future habitat loss in regions such as the confluence of the Sacramento and San Joaquin Rivers where the delta smelt typically inhabit.<sup>38</sup> In 2016, Brown and colleagues also found that the overall number of days of stressful temperature conditions will increase to >60 days for >50% of location across the delta by the end of the century.<sup>25</sup> Combining long-term data records with global climate models may help further constrain projections of expected impacts on vulnerable species habitat. Importantly, Brown et al. 2016 also shows that the investigation of sublethal conditions (24 °C) may provide a more realistic view into how habitat stress and the gradual onset of temperature-related declines on the delta smelt that may arise due to rising temperatures prior to reaching predominantly lethal conditions.<sup>25</sup>

In this study, we apply a more conservative approach by leveraging thermal tolerance thresholds ( $CT_{\text{max}}$ ) established in a laboratory-controlled study led by Davis and colleagues<sup>22</sup> to estimate areas of  $TUH$ , although it is important to note that the delta smelt are rarely observed under  $CT_{\text{max}}$  conditions. The maps of the annual maximum WST are shown for 1996, the low point of the unsuitability signals, and 2017, the high point of unsuitable habitat, in Figure S1. Non-native species, such as the largemouth bass and Mississippi silverside can tolerate water temperatures at least 4.7 °C higher, allowing them to out-compete the delta smelt under increases in the

$TUH$  relative to the delta smelt  $CT_{\text{max}}$  (28.6 °C). This may be further exacerbated by the fact that the delta smelt are considered prey to these non-natives.<sup>39</sup>

It is also important to note that surface temperature conditions can vary substantially from bulk temperature conditions in the subsurface aquatic habitat, a phenomenon often referred to as the skin effect.<sup>34,40,41</sup> Differences between surface or skin temperatures in comparison with bulk temperatures can be as high as 5 °C with modeled estimates in the delta indicating regional dependencies in the varying temperature conditions within the water column.<sup>42,43</sup> Although previous studies note strong seasonal and diurnal dependencies on the skin effect,<sup>34,42</sup> this study relies on annual maximums of surface water temperatures, acquired at the same local time each day, to examine longer-term trends (1985–2019) in  $TUH$ . The maximum temperatures considered in this study are conservative values because the morning overpass of Landsat does not observe the warmest time of day. This study focuses on implications of increasing long-term trends in water temperature conditions on vulnerable aquatic species, such as the delta smelt. Future work understanding how surface temperatures are related to bulk temperatures in the delta may help bridge the use of remotely sensed surface temperatures with shorter-term planning and mitigation efforts such as habitat restoration. ECOSystem Spaceborne Thermal Radiometer Experiment on Space Station (ECOSTRESS), a thermal instrument on-board the International Space Station, provides higher resolution (70 m pixels, 1–5 day revisit, and variable acquisition times) surface temperature measurements that can be used in combination with in situ station data to better characterize controls on the skin effect in the delta, enabling future applications of remotely sensed surface temperatures to be used to estimate bulk temperatures. This may also enable custom applications seeking to mitigate thermal stressors on the delta smelt, such as identifying or establishing areas of thermal refuges.

**Relationship Between Surface Temperature and Abundance.** There is an inverse relationship between  $TUH_{\text{smelt}}$  and the delta smelt abundance index, as shown in

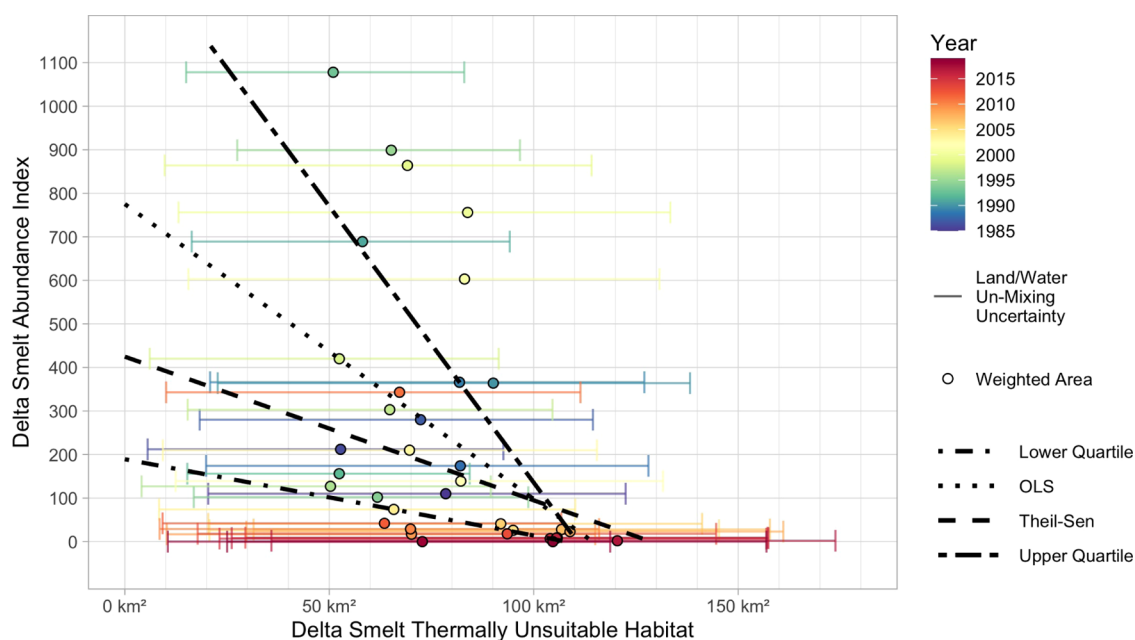


**Figure 6.** Scatterplot of delta smelt abundance index and  $TUH_{smelt}$  with lower quartile, Theil–Sen, and upper quartile lines, forming a limiting factor wedge. The points represent weighted areas, and the horizontal error bars display the upper and lower bounds of land/water unmixing.

the Figure 5 timeline as well as the Figure 6 scatter-plot with Theil–Sen and quartile trends. We found strong negative correlations using Pearson ( $r = -0.44$ ,  $p < 0.01$ ), Spearman ( $\rho = -0.58$ ,  $p < 0.01$ ), and Kendall ( $\tau = -0.4$ ,  $p < 0.01$ ) methods and a moderate OLS coefficient of determination ( $R^2 = 0.2$ ,  $p < 0.01$ ). This  $R^2$  is a conservative metric, due to the nonlinear relationship of abundance and TUH. We take this  $R^2$  to mean that the remotely sensed thermal stress is able to explain about one-fifth of the annual variation in the delta smelt population. We consider this a preliminary estimate of the influence thermal habitat suitability has on abundance. Recent advances in high-resolution remote sensing of turbidity and their effects on the delta smelt habitat have also recently been explored.<sup>44,45</sup> We intend to further refine this quantification of the effect that temperature has on the delta smelt through multivariate analysis, taking turbidity and other water quality factors into account in future work. The OLS line intercepts the  $TUH_{smelt}$  axis at  $114 \text{ km}^2$ . The Theil–Sen trend line intercepts the TUH axis at  $129 \text{ km}^2$ , just past the all-time high of  $120 \text{ km}^2$ . The lower and upper quartile lines intercept the TUH<sub>smelt</sub> axis near the Theil–Sen line at  $107 \text{ km}^2$  and  $111 \text{ km}^2$ , respectively. Abundances are near zero when  $TUH_{smelt}$  is in the range of these intercepts from  $107$  to  $129 \text{ km}^2$ . The delta smelt are unlikely to thrive in any future years when more than  $107 \text{ km}^2$  of habitat reach a temperature exceeding  $28.6 \text{ }^\circ\text{C}$ .

There have been many studies focused on identifying and quantifying the causes of the delta smelt decline in the SFE. Modeling studies have identified multiple factors that predict the delta smelt abundance including water clarity,<sup>46</sup> winter exports, the isohaline position in the estuary, warmer summer temperatures, and biotic factors including predator–prey interactions.<sup>47–49</sup> Mechanistic life cycle models suggest that no single factor is responsible for delta smelt abundances, and it is likely that different factors (e.g., temperature, hydrodynamic/entrainment at pumps, predation and competition, and food availability and possibly others) are limiting at different life stages<sup>50,51</sup> and across different life-history phenotypes.<sup>52</sup> Quantile regression has been demonstrated to

be an effective approach to characterizing fish habitat limitations in the presence of multiple, often unquantified limiting factors.<sup>53–55</sup> In this study, the wedge-shaped pattern in Figure 6 indicates that the area of TUH is a limiting factor for delta smelt abundance, even if other limiting conditions have not been fully characterized. At low amounts of TUH area, smelt abundances are likely limited by other habitat factors and biotic processes. As the amount of TUH increases and becomes the dominant limiting factor, low abundances occur, even if other habitat conditions and biotic factors may be optimal,<sup>55</sup> with near-zero abundances occurring past  $107 \text{ km}^2$  (Figure 6).

The  $WST_{max}$  measure of delta smelt aquatic habitat temperature is increasing by  $0.1 \text{ }^\circ\text{C}$  per year ( $p < 0.01$ ), according to Theil–Sen regression, with a significant trend according to Mann–Kendall ( $\tau = 0.56$ ,  $p < 0.01$ ), as displayed in Figure S2 and Table S3. The coolest year of 1992, with a  $WST_{max}$  of  $20.22 \text{ }^\circ\text{C}$ , precedes the largest increase in delta smelt abundance from 156 to 1078 in 1993 (Table S3). The warmest year in the Landsat record occurred in 2017 with a  $WST_{max}$  of  $26.07 \text{ }^\circ\text{C}$ , and the following year in 2018 was the first year with zero abundance index for the delta smelt. The increasing trend in  $WST_{max}$  and  $TUH_{smelt}$  and the inverse relationship between  $TUH_{smelt}$  and delta smelt abundance index suggest that temperatures are rising in the delta smelt habitat and that warming waters are reducing the available habitat for the delta smelt.

## FUTURE WORK

The findings regarding the fish habitat presented in this study apply only to the water surface and only to the approximately 10:30 AM overpass of the Landsat satellites. To better assess the aquatic habitat, a future study will examine subsurface bulk temperatures measured throughout the day and compare them to diurnal WST seen by ECOSTRESS. ECOSTRESS was not included in this analysis because its period of coverage from 2018 is too short to compare to the Landsat record, but ECOSTRESS can uniquely capture the mid-day maximum of

surface temperature that cannot be acquired by Landsat. This opportunity to better understand the diurnal WST and its relationship to bulk water temperature will be explored by the Research Opportunities in Space and Earth Sciences 2018 (ROSES) ECOSTRESS Science and Applications Team.<sup>56</sup>

## ■ ASSOCIATED CONTENT

### SI Supporting Information

The Supporting Information is available free of charge at <https://pubs.acs.org/doi/10.1021/acs.est.1c02837>.

Maps demonstrating best and worst years for delta smelt habitat, table of species studied and their thermal tolerances, graph of habitat temperature trend, and table of habitat quantification by year (PDF)

## ■ AUTHOR INFORMATION

### Corresponding Author

**Gregory H. Halverson** – NASA Jet Propulsion Laboratory, California Institute of Technology, Pasadena, California 91109, United States; [orcid.org/0000-0002-4028-4357](https://orcid.org/0000-0002-4028-4357); Email: [gregory.h.halverson@jpl.nasa.gov](mailto:gregory.h.halverson@jpl.nasa.gov)

### Authors

**Christine M. Lee** – NASA Jet Propulsion Laboratory, California Institute of Technology, Pasadena, California 91109, United States

**Erin L. Hestir** – University of California, Merced, Merced, California 95343, United States

**Glynn C. Hulley** – NASA Jet Propulsion Laboratory, California Institute of Technology, Pasadena, California 91109, United States

**Kerry Cawse-Nicholson** – NASA Jet Propulsion Laboratory, California Institute of Technology, Pasadena, California 91109, United States

**Simon J. Hook** – NASA Jet Propulsion Laboratory, California Institute of Technology, Pasadena, California 91109, United States

**Brian A. Bergamaschi** – USGS California Water Science Center, Sacramento, California 95819, United States

**Shawn Acuña** – Metropolitan Water District of Southern California, Sacramento, California 95814, United States

**Nicholas B. Tuffillaro** – Oregon State University, Corvallis, Oregon 97331, United States

**Robert G. Radocinski** – NASA Jet Propulsion Laboratory, California Institute of Technology, Pasadena, California 91109, United States

**Gerardo Rivera** – NASA Jet Propulsion Laboratory, California Institute of Technology, Pasadena, California 91109, United States

**Ted R. Sommer** – California Department of Water Resources, Sacramento, California 95814, United States

Complete contact information is available at: <https://pubs.acs.org/doi/10.1021/acs.est.1c02837>

### Notes

The authors declare no competing financial interest.

## ■ ACKNOWLEDGMENTS

The research described in this paper was carried out at the Jet Propulsion Laboratory, California Institute of Technology, under contract with the National Aeronautics and Space Administration, NNH16ZDA001N-WATER. 2021 California

Institute of Technology. Government sponsorship acknowledged.

## ■ REFERENCES

- (1) Jay, A.; Reidmiller, D.; Avery, C.; Barrie, D.; DeAngelo, B.; Dave, A.; Kolian, M.; Lewis, K.; Reeves, K.; Winner, D.; Dzaugis, M. *Fourth National Climate Assessment*; U.S. Global Change Research Program, 2018.
- (2) Akbari, E.; Alavipanah, S. K.; Jeihouni, M.; Hajeb, M.; Haase, D.; Alavipanah, S. A review of ocean/sea subsurface water temperature studies from remote sensing and non-remote sensing methods. *Water (Switzerland)* **2017**, *9*, 936.
- (3) Schaeffer, B. A.; Iames, J.; Dwyer, J.; Urquhart, E.; Salls, W.; Rover, J.; Seegers, B. An initial validation of Landsat 5 and 7 derived surface water temperature for U.S. lakes, reservoirs, and estuaries. *Int. J. Rem. Sens.* **2018**, *39*, 7789–7805.
- (4) Malakar, N. K.; Hulley, G. C.; Hook, S. J.; Laraby, K.; Cook, M.; Schott, J. R. An Operational Land Surface Temperature Product for Landsat Thermal Data: Methodology and Validation. *IEEE Trans. Geosci. Rem. Sens.* **2018**, *56*, 5717–5735.
- (5) Conomos, T. J. *Pacific Division*; American Association for the Advancement of Science, 1979; p 493.
- (6) Nichols, F. H.; Cloern, J. E.; Luoma, S. N.; Peterson, D. H. The modification of an estuary. *Science* **1986**, *231*, 567–573.
- (7) USGS. Delta Subsidence in California. <https://pubs.usgs.gov/fs/2000/fs00500/pdf/fs00500.pdf> (accessed July 14, 2021).
- (8) Delta Stewardship Council. *The Delta Plan: Ensuring a Reliable Water Supply for California, a Healthy Delta Ecosystem, and a Place of Enduring Value 2013 Contents*, 2013.
- (9) Myers, N.; Mittermeier, R. A.; Mittermeier, C. G.; Da Fonseca, G. A. B.; Kent, J. Biodiversity hotspots for conservation priorities. *Nature* **2000**, *403*, 853–858.
- (10) Center for Biological Diversity. San Francisco Bay Area and Delta Protection. [https://www.biologicaldiversity.org/campaigns/san\\_francisco\\_bay\\_area\\_and\\_delta\\_protection/index.html](https://www.biologicaldiversity.org/campaigns/san_francisco_bay_area_and_delta_protection/index.html) (accessed July 14, 2021).
- (11) Luoma, S. N.; Dahm, C. N.; Healey, M.; Moore, J. N. Challenges facing the Sacramento-San Joaquin Delta: Complex, chaotic, or simply cantankerous? *San Franc. Estuary Watershed Sci.* **2015**, *13*, 1–25.
- (12) Cloern, J. E.; Knowles, N.; Brown, L. R.; Cayan, D.; Dettinger, M. D.; Morgan, T. L.; Schoellhamer, D. H.; Stacey, M. T.; van der Wegen, M.; Wagner, R. W.; Jassby, A. D. Projected Evolution of California's San Francisco Bay-Delta-River System in a Century of Climate Change. *PLoS One* **2011**, *6*, No. e24465.
- (13) Ustin, S. L.; Santos, M. J.; Hestir, E. L.; Khanna, S.; Casas, A.; Greenberg, J. Developing the capacity to monitor climate change impacts in Mediterranean estuaries. *Evol. Ecol. Res.* **2014**, *16*, 529–550.
- (14) Hestir, E. L.; Khanna, S.; Andrew, M. E.; Santos, M. J.; Viers, J. H.; Greenberg, J. A.; Rajapakse, S. S.; Ustin, S. L. Identification of invasive vegetation using hyperspectral remote sensing in the California Delta ecosystem. *Remote Sens. Environ.* **2008**, *112*, 4034–4047.
- (15) Khanna, S.; Santos, M. J.; Boyer, J. D.; Shapiro, K. D.; Bellvert, J.; Ustin, S. L. Water primrose invasion changes successional pathways in an estuarine ecosystem. *Ecosphere* **2018**, *9*, No. e02418.
- (16) Brooks, M. L.; Fleishman, E.; Brown, L. R.; Lehman, P. W.; Werner, I.; Scholz, N.; Mitchelmore, C.; Lovvorn, J. R.; Johnson, M. L.; Schlenk, D.; van Drunick, S.; Drever, J. I.; Stoms, D. M.; Parker, A. E.; Dugdale, R. Life Histories, Salinity Zones, and Sublethal Contributions of Contaminants to Pelagic Fish Declines Illustrated with a Case Study of San Francisco Estuary, California, USA. *Estuar. Coast* **2012**, *35*, 603–621.
- (17) Grimaldo, L. F.; Sommer, T.; Van Ark, N.; Jones, G.; Holland, E.; Moyle, P. B.; Herbold, B.; Smith, P. Factors Affecting Fish Entrainment into Massive Water Diversions in a Tidal Freshwater Estuary: Can Fish Losses be Managed? *N. Am. J. Fish. Manag.* **2009**, *29*, 1253–1270.

- (18) Hutton, P. H.; Rath, J. S.; Chen, L.; Unga, M. J.; Roy, S. B. Nine Decades of Salinity Observations in the San Francisco Bay and Delta: Modeling and Trend Evaluations. *J. Water Resour. Plann. Manag.* **2016**, *142*, 04015069.
- (19) United States Fish and Wildlife Service. ECOS: USFWS Threatened and Endangered Species Active Critical Habitat Report. <https://ecos.fws.gov/ecp/report/table/critical-habitat.html> (accessed July 14, 2021).
- (20) Sommer, T.; Armor, C.; Baxter, R.; Breuer, R.; Brown, L.; Chotkowski, M.; Culberson, S.; Feyrer, F.; Gingras, M.; Herbold, B.; Kimmerer, W.; Mueller-Solger, A.; Nobriga, M.; Souza, K. The Collapse of Pelagic Fishes in the Upper San Francisco Estuary: El Colapso de los Peces Pelagicos en La Cabecera Del Estuario San Francisco. *Fisheries* **2007**, *32*, 270–277.
- (21) Moyle, P. B.; Brown, L. R.; Durand, J. R.; Hobbs, J. A. Delta smelt: Life history and decline of a once-abundant species in the San Francisco estuary. *San Franc. Estuary Watershed Sci.* **2016**, *14*, 1–30.
- (22) Davis, B. E.; Cocherell, D. E.; Sommer, T.; Baxter, R. D.; Hung, T.-C.; Todgham, A. E.; Fanguie, N. A. Sensitivities of an endemic, endangered California smelt and two non-native fishes to serial increases in temperature and salinity: implications for shifting community structure with climate change. *Conserv. Physiol.* **2019**, *7*, coy076.
- (23) Hasenbein, M.; Komoroske, L. M.; Connon, R. E.; Geist, J.; Fanguie, N. A. Turbidity and salinity affect feeding performance and physiological stress in the endangered delta smelt. *Integr. Comp. Biol.* **2013**, *53*, 620–634.
- (24) Sommer, T.; Mejia, F. H.; Nobriga, M. L.; Feyrer, F.; Grimaldo, L. The Spawning Migration of Delta Smelt in the Upper San Francisco Estuary. *San Franc. Estuary Watershed Sci.* **2011**, *9*, 1–16.
- (25) Brown, L. R.; Komoroske, L. M.; Wagner, R. W.; Morgan-King, T.; May, J. T.; Connon, R. E.; Fanguie, N. A. Coupled downscaled climate models and ecophysiological metrics forecast habitat compression for an endangered estuarine fish. *PLoS One* **2016**, *11*, No. e0146724.
- (26) Wagner, R. W.; Stacey, M.; Brown, L. R.; Dettinger, M. Statistical Models of Temperature in the Sacramento-San Joaquin Delta Under Climate-Change Scenarios and Ecological Implications. *Estuar. Coast* **2011**, *34*, 544–556.
- (27) Yang, J.; Gong, P.; Fu, R.; Zhang, M.; Chen, J.; Liang, S.; Xu, B.; Shi, J.; Dickinson, R. The role of satellite remote sensing in climate change studies. *Nat. Clim. Change* **2013**, *3*, 875–883.
- (28) Hulley, G.; Rivera, G.; Radocinski, R.; Hook, S.; Arab, R. D. Landsat surface temperature (ST) validation. In *Landsat Science Team Meeting, 4–6 February 2020*; 2020.
- (29) Schott, J. R.; Hook, S. J.; Barsi, J. A.; Markham, B. L.; Miller, J.; Padula, F. P.; Raqueno, N. G. Thermal infrared radiometric calibration of the entire Landsat 4, 5, and 7 archive (1982–2010). *Remote Sens. Environ.* **2012**, *122*, 41–49.
- (30) Barsi, J. A.; Markham, B. L.; Schott, J. R.; Hook, S. J.; Raqueno, N. G. Twenty-five years of landsat thermal band calibration. *2010 IEEE International Geoscience and Remote Sensing Symposium*; IEEE, 2010; pp 2287–2290.
- (31) Survey USG. USGS/EROS Inventory Service Documentation (Machine-to-Machine API). 2020. <https://m2m.cr.usgs.gov/> (accessed July 14, 2021).
- (32) Martí-Cardona, B.; Prats, J.; Niclòs, R. Enhancing the retrieval of stream surface temperature from Landsat data. *Remote Sens. Environ.* **2019**, *224*, 182–191.
- (33) NASA Jet Propulsion Laboratory. Welcome to Salton Sea — Welcome to Salton Sea Validation. <https://saltonsea.jpl.nasa.gov/> (accessed July 14, 2021).
- (34) Wilson, R. C.; Hook, S. J.; Schneider, P.; Schladow, S. G. Skin and bulk temperature difference at Lake Tahoe: A case study on lake skin effect. *J. Geophys. Res. Atmos.* **2013**, *118*, 332.
- (35) California Department of Fish and Wildlife. Fall Midwater Trawl. <https://www.dfg.ca.gov/delta/projects.asp?ProjectID=FMWT> (accessed July 14, 2021).
- (36) California Department of Fish and Wildlife. *Monthly Abundance Indices*, 2019.
- (37) Cade, B. S.; Terrell, J. W.; Schroeder, R. L. Estimating effects of limiting factors with regression quantiles. *Ecology* **1999**, *80*, 311–323.
- (38) Brown, L. R.; Bennett, W. A.; Wagner, R. W.; Morgan-King, T.; Knowles, N.; Feyrer, F.; Schoellhamer, D. H.; Stacey, M. T.; Dettinger, M. Implications for Future Survival of Delta Smelt from Four Climate Change Scenarios for the Sacramento-San Joaquin Delta, California. *Estuar. Coast* **2013**, *36*, 754–774.
- (39) Schreier, B. M.; Baerwald, M. R.; Conrad, J. L.; Schumer, G.; May, B. Examination of Predation on Early Life Stage Delta Smelt in the San Francisco Estuary Using DNA Diet Analysis. *Trans. Am. Fish. Soc.* **2016**, *145*, 723–733.
- (40) Minnett, P. J.; Smith, M.; Ward, B. Measurements of the oceanic thermal skin effect. *Deep Sea Res., Part II* **2011**, *58*, 861–868.
- (41) Minnett, P. J. Radiometric measurements of the sea-surface skin temperature: The competing roles of the diurnal thermocline and the cool skin. *Int. J. Rem. Sens.* **2003**, *24*, 5033–5047.
- (42) Nehorai, R.; Lensky, N.; Brenner, S.; Lensky, I. The dynamics of the skin temperature of the dead sea. *Advances in Meteorology* **2013**, *2013*, 1–9.
- (43) Vroom, J.; van der Wegen, M.; Martyr-Koller, R. C.; Lucas, L. V. What Determines Water Temperature Dynamics in the San Francisco Bay-Delta System? *Water Resour. Res.* **2017**, *53*, 9901–9921.
- (44) Lee, C. M.; Hestir, E. L.; Tuffiaro, N.; Palmieri, B.; Acuña, S.; Osti, A.; Bergamaschi, B. A.; Sommer, T. Monitoring Turbidity in San Francisco Estuary and Sacramento–San Joaquin Delta Using Satellite Remote Sensing. *J. Am. Water Resour. Assoc.* **2021**, *57*, 737–751.
- (45) Ade, C.; Hestir, E. L.; Lee, C. M. Assessing Fish Habitat and the Effects of an Emergency Drought Barrier on Estuarine Turbidity Using Satellite Remote Sensing. *J. Am. Water Resour. Assoc.* **2021**, *57*, 752–770.
- (46) Thomson, J. R.; Kimmerer, W. J.; Brown, L. R.; Newman, K. B.; Nally, R. M.; Bennett, W. A.; Feyrer, F.; Fleishman, E. Bayesian change point analysis of abundance trends for pelagic fishes in the upper San Francisco Estuary. *Ecol. Appl.* **2010**, *20*, 1431–1448.
- (47) Mac Nally, R.; Thomson, J. R.; Kimmerer, W. J.; Feyrer, F.; Newman, K. B.; Sih, A.; Bennett, W. A.; Brown, L.; Fleishman, E.; Culberson, S. D.; Castillo, G. Analysis of pelagic species decline in the upper San Francisco Estuary using multivariate autoregressive modeling (MAR). *Ecol. Appl.* **2010**, *20*, 1417–1430.
- (48) Maunder, M. N.; Deriso, R. B. A state-space multistage life cycle model to evaluate population impacts in the presence of density dependence: Illustrated with application to delta smelt (*Hypomesus transpacificus*). *Can. J. Fish. Aquat. Sci.* **2011**, *68*, 1285–1306.
- (49) Miller, W. J.; Manly, B. F. J.; Murphy, D. D.; Fullerton, D.; Ramey, R. R. An Investigation of Factors Affecting the Decline of Delta Smelt (*Hypomesus transpacificus*) in the Sacramento-San Joaquin Estuary. *Rev. Fish. Sci.* **2012**, *20*, 1–19.
- (50) Rose, K. A.; Kimmerer, W. J.; Edwards, K. P.; Bennett, W. A. Individual-based modeling of delta smelt population dynamics in the upper san francisco estuary: I. model description and baseline results. *Trans. Am. Fish. Soc.* **2013**, *142*, 1238–1259.
- (51) Hamilton, S. A.; Murphy, D. D. Analysis of Limiting Factors Across the Life Cycle of Delta Smelt (*Hypomesus transpacificus*). *Environ. Manag.* **2018**, *62*, 365–382.
- (52) Hobbs, J. A.; Lewis, L. S.; Willmes, M.; Denney, C.; Bush, E. Complex life histories discovered in a critically endangered fish. *Sci. Rep.* **2019**, *9*, 16772.
- (53) Terrell, J. W.; Cade, B. S.; Carpenter, J.; Thompson, J. M. Modeling Stream Fish Habitat Limitations from Wedge-Shaped Patterns of Variation in Standing Stock. *Trans. Am. Fish. Soc.* **1996**, *125*, 104–117.
- (54) Cade, B. S.; Noon, B. R. A gentle introduction to quantile regression for ecologists. *Front. Ecol. Environ.* **2003**, *1*, 412–420.
- (55) Schmidt, T. S.; Clements, W. H.; Cade, B. S. Estimating risks to aquatic life using quantile regression. *Freshw. Sci.* **2012**, *31*, 709–723.

(56) ECOSTRESS Science and Applications Team. <https://nspires.nasaprs.com/external/solicitations/summary!init.do?solId=\\%7B7A765554-13CD-C6BA-A628-F4675EC9DEE2\\%7D&path=open> (accessed July 14, 2021).

**HAZARD AWARENESS  
REDUCES LAB INCIDENTS**

**ACS Essentials of  
Lab Safety for  
General Chemistry**

A new course from the  
American Chemical Society

ACS Institute  
Learn. Develop. Excel.

EXPLORE  
ORGANIZATIONAL  
SALES  
[solutions.acs.org/essentialsoflabsafety](https://solutions.acs.org/essentialsoflabsafety)

REGISTER FOR  
INDIVIDUAL ACCESS  
[institute.acs.org/courses/essentials-lab-safety.html](https://institute.acs.org/courses/essentials-lab-safety.html)